



Pharmacodynamic evaluation and network pharmacology analysis of a novel anti-heat stress Chinese herbal formula

Hanfei Wang¹, Shuyi Xu¹, Haiyang Mao¹, Boyu Wang¹, Yanping Feng², Awais Ihsan³, Shijun Li^{2,4,5*} and Xu Wang^{1*} 

Abstract

Frequent extreme heat events around the world not only pose a major threat to human health but also cause significant economic losses to the livestock industry. The existing management practices are insufficient to fully prevent heat stress with an urgent need to develop preventive medicines. The aim of this study was to develop an anti-heat stress Chinese herbal formula (CHF) via big data analysis techniques and to evaluate its anti-heat stress effect and mechanism of action *via* pharmacodynamic evaluation and network pharmacology analysis. Many anti-heat stress CHFs were collected from the Chinese National Knowledge Infrastructure (CNKI) database. Three alternative CHFs were obtained via unsupervised entropy hierarchical clustering analysis, and the most effective CHF against heat stress, Shidi Jieshu decoction (SJD), was obtained by screening in a mouse heat stress model. In dry and hot environments, SJD significantly improved the heat tolerance of AA broilers by 4–6°C. In a humid and hot environment, pretreatment with 2% SJD resulted in 100% survival of Wenchang chickens at high temperatures. The main active ingredients of SJD were identified as muntjacoside E, timosaponin C, macrostemonoside H and mangiferin *via* ultra-performance liquid chromatography/mass spectrometry (UPLC/MS) and database comparison. The active ingredients of SJD were found to target tumor necrosis factor- α (TNF- α), signal transducer activator of transcription 3 (STAT3) and epidermal growth factor receptor (EGFR). Finally, the safety of the new formulation was assessed in an acute oral toxicity study in rats. The SJDs developed in this study provide a new option for the prevention of heat stress in animal husbandry and offer new insights for further research on anti-heat stress.

Highlights

1. Shidi Jieshu decoction (SJD) increases the heat tolerance of animals.
2. SJD increased the survival rate of Wenchang chickens under heat stress to 100%.
3. SJD can be used to prevent heat stress in animals and humans.
4. EGFR and STAT3 may be novel anti-heat stress targets in addition to inflammation.

Keywords Hot weather, Heat stress, Big data analysis technology, Network pharmacology, Molecular docking, Chicken

Handling Editor: Zhixin Lei.

*Correspondence:

Shijun Li

lishijun@mail.hzau.edu.cn

Xu Wang

wangxu@mail.hzau.edu.cn

Full list of author information is available at the end of the article

Introduction

The frequency and severity of extreme heat events are increasing worldwide (Mu et al. 2022). According to the World Meteorological Organization (WMO), the Earth experienced its hottest summer on record in 2023, with temperatures soaring and even sea surface temperatures



© The Author(s) 2024. **Open Access** This article is licensed under a Creative Commons Attribution 4.0 International License, which permits use, sharing, adaptation, distribution and reproduction in any medium or format, as long as you give appropriate credit to the original author(s) and the source, provide a link to the Creative Commons licence, and indicate if changes were made. The images or other third party material in this article are included in the article's Creative Commons licence, unless indicated otherwise in a credit line to the material. If material is not included in the article's Creative Commons licence and your intended use is not permitted by statutory regulation or exceeds the permitted use, you will need to obtain permission directly from the copyright holder. To view a copy of this licence, visit <http://creativecommons.org/licenses/by/4.0/>. The Creative Commons Public Domain Dedication waiver (<http://creativecommons.org/publicdomain/zero/1.0/>) applies to the data made available in this article, unless otherwise stated in a credit line to the data.

reaching unprecedented highs. Data from the China Climate Bulletin (2022) revealed that China's climate in 2022 was markedly warm and dry, with a national average temperature of 10.51°C, which is 0.62°C higher than normal and the second highest on record, and the year's extremely high-temperature events were the highest on record. At elevated temperatures, heat-related illnesses such as heatstroke, heat cramps or heat exhaustion are common, with heatstroke being the most prevalent and resulting in a mortality rate of up to 20%, even with prompt treatment. Prolonged exposure to high temperatures has the potential to trigger physiological mechanisms such as ischemia, inflammatory responses and rhabdomyolysis, and many other vital organs, such as the brain, heart and liver, can be severely affected (Mora et al. 2017; Munguia et al. 2024; Umemura et al. 2018).

Heat waves not only have a negative impact on human health but also have an adversely impact agricultural production (Gonzalez-Rivas et al. 2020; Nawab et al. 2018; Saeed et al. 2019). The protein content of wheat and the yield of all cereals significantly decrease as the temperature increases (Asseng et al. 2019). In Australia, approximately 21,000 sheep are potentially at risk of dying from heat stress (a physiological state in which body heat exceeds dissipation capacity, raising core temperature) during the mating season, which would result in a considerable annual loss of \$97 million to the Australian wool industry (van Wettere et al. 2021). Animal heat stress due to high temperatures causes annual losses of \$128-165 million in the poultry industry, with annual economic losses due to animal heat stress reaching \$1.69-2.36 billion in the U.S. livestock industry (Vandana et al. 2021). In summary, the increasing severity of global heat waves poses a significant threat to human health and ecosystems while causing significant losses to the livestock industry.

Heat stress disrupts the homeostasis of free radicals in an organism, leading to alterations in protein, lipid and energy metabolism and ultimately affecting the production, reproduction and health status of the animal (Sejian et al. 2018; Zheng et al. 2021). A typical manifestation of heat stress is a decrease in feed intake, resulting in a decrease in feed intake and growth rate as the ambient temperature increases, leading to a decrease in growth performance (Godde et al. 2021; Ma et al. 2021). In addition, heat stress increases oxidative reactions in livestock and poultry, leading to increased mortality (Surai et al. 2019). Under high heat conditions, reactive oxygen species (ROS) are overproduced in the organism, and oxidative stress occurs in livestock and poultry when their levels exceed the antioxidant capacity in the organism (Dadgar et al. 2021). For example, oxidative reactions that occur in broilers under heat stress affect muscle pH, water retention and tenderness, ultimately affecting the

quality of the meat produced (Shakeri et al. 2019). Heat stress also affects livestock production by reducing animal fertility. Cattle have been shown to be less sperm active at high heat and more prone to multiple sperm fertilizations during insemination (Pernas et al. 2023). Heat stress also increases sperm DNA fragmentation in rams, and fragmentation is highly likely to cause sterility (Hamilton et al. 2018). Nevertheless, the therapeutic target of heat stress is unknown, although the association between heat shock proteins and heat stress has long been reported but are considered poor therapeutic targets because they exacerbate more terminal events as target markers (e.g., cytotoxicity, inflammation and coagulation responses) (Gomez-Pastor et al. 2018; Sedaghatmehr et al. 2021). Recent studies suggest that the cardiovascular and pulmonary systems are the main systems affected by heat stress, but the mechanism is still unknown (Chen et al. 2019; Nan et al. 2023).

The assessment and prevention of heat stress hazards, as well as the study of heat stress response mechanisms, are among the most important areas of research on the resilience of livestock and poultry to extreme heat. Currently, the main measures used to prevent heat stress in livestock and poultry include physical cooling, nutritional regulation and genetic breeding. However, these options are not effective enough to prevent and alleviate heat stress in livestock and poultry (Asseng et al. 2021; Desta 2021; Fathi et al. 2022; Wickramasuriya et al. 2019). The systemic therapeutic concept and low production cost of Chinese herbal formulas (CHF) give them high potential to prevent heat stress. For example, Huoxiang Zhengqi Dropping Pill (HZDP), which originated from the ancient Chinese pharmacy book *Taiping Huimin Hejiju Fang*, is widely used to prevent heat stroke in people in summer, but the irritating odor has limited its use in animal husbandry (Li et al. 2022). In this study, with the help of big data analysis technology, we developed an anti-heat stress traditional CHF, which effectively improved the survival rate of mice and chickens in high-temperature environments. The survival rate of Wenchang chickens in high-temperature environments could reach 100% with preventive the administration of medicine in advance, which provides a reference for the application of this formula. Furthermore, we used network pharmacology to investigate the mechanism of heat stress resistance in CHF patients, which provides a theoretical basis for heat stress resistance research.

Results

Big data analysis of the anti-heat stress effects of herbs

By searching the CNKI database for articles on CHF about the detection and treatment of heat stress from 1 January 2001 to 1 December 2023, a total of 490 articles

were obtained (Fig. 1A). After further screening and exclusion, a total of 50 CHF were included. The basic information of these 50 CHF was obtained after they were incorporated into the Chinese Medicine Inheritance Auxiliary Platform (V2.5) (CMIAP). According to the classification of the four natures, the drugs in these 50 CHF were mainly cold, warm or moderate (Fig. 1B). The five flavors were classified as sweet, bitter or spicy (Fig. 1C). The meridian tropisms were located mainly on the stomach meridian, lung meridian, spleen meridian and heart meridian (Fig. 1D). The frequency statistics of the drugs in these 50 CHF revealed that the top 3 herbs with the highest frequency of use were liquorice, *Scutellariae radix* and mosla herb (Fig. 1E).

Screening of new CHF for anti-heat stress

Using CMIAP, we formulated new CHF for anti-heat stress. Unsupervised entropy hierarchical cluster analysis was performed on the 50 entered CHF, and three new heat stress CHF were obtained (Fig. 1F), named F1, F2 and F3, which were given to different groups of mice by oral gavage for 1 h and then heat-treated, starting at 45°C and increasing by 1°C every 10 min (Fig. 1G) Until mice in all the groups died, and the survival time of the mice in each group was calculated.

All the mice in the control group died when the temperature was raised to 48°C, whereas all the mice in groups F1, F2 and F3 died at 50°C, with the mice in group F1 surviving the longest (Fig. 1H). Histological analysis of the hearts, lungs and livers of the mice in the control and F1 groups revealed that the control mice had unclear cardiac transverse striations, vacuolated myocardium (indicated by arrows) and myocardial fiber breaks, whereas myocardial vacuolation and myocardial fiber breaks were significantly reduced in the F1 group (Fig. 1I). The lungs of the control mice showed obvious hemorrhage, blurred alveolar structure and marked thickening of the alveolar septa (indicated by arrows); the alveolar structure of the F1 group mice was clearer, and the alveolar septa were less thickened. In the control mice, the liver showed obvious hemorrhage, with many blood cells in

the hepatic sinusoids leaking into the liver parenchyma, the integrity of the blood vessel wall in the sinusoids was impaired, and the endothelial cells of blood vessel were vacuolated. In the F1 group, although there was also liver hemorrhage, no blood cells were found in the liver sinusoids and only a few blood cells were in the mesenchymal spaces (indicated by arrows). In conclusion, these results suggest that the newly formulated formulas F1, F2 and F3 all have better anti-heat stress effects, with F1 having the best anti-heat stress effect, and it is possible that F1 can significantly alleviate organ damage caused by high temperatures and has better protective effects on the heart, lungs and liver.

The acute heat stress model of high temperature and dryness was used to verify the protective effect of F1 on broilers

Since the summer high-temperature weather conditions are different in different regions of China, simulations have been made to measure the anti-heat stress effect of F1 under different high-temperature environments, with reference data acquired from the China Meteorological Data Network (<http://data.cma.cn/>). The data revealed the weather changes in Turpan (Xinjiang Province), a city in northwest China, over the years and the extremely high temperatures in Turpan from April to September reached 39.4–47.7°C, with a humidity of approximately 25–39% (Fig. 2A). To expedite the test, the minimum temperature was set at 57°C with humidity and the AA broilers were heat-treated after gavage while increasing the temperature by 1°C every 10 min until all the broilers died (Fig. 2C).

The Chinese herbal formula F1 with the optimal anti-heat stress effect obtained from the previous screening was named Shidi Jieshu Decoction (SJD). We gavaged broilers with three doses of SJD: high (designated SJD-H, gavaged with the original SJD solution), medium (designated SJD-M, gavaged with 10% SJD) and low (designated SJD-L, gavaged with 1% SJD), and the control group of broilers was gavaged with an equal volume of distilled water. Prior to the experiment, the broilers in each group

(See figure on next page.)

Fig. 1 Process of big data analysis and basic information of CHF and screening of anti-heat stress CHF. **A** Process of big data analysis of herbal formulas for the treatment of heat stress. The medicines of the 50 CHF included in this study were analyzed for **(B)** four natures, **(C)** five flavors, and **(D)** meridian tropism. **E** Drug frequency statistics of the drugs in the CHF included in this study. The greater the frequency of the use of Chinese herbal medicine in the word cloud diagram is, the greater the number of names represented. **F** Three new CHF. **G** Construction of a heat stress mouse model for screening CHF. **H** Survival rate of mice under acute heat stress, $n=10$. **I** Histological analysis of the hearts, lungs and livers of the mice. The arrows indicate vacuolization and rupture of the myocardium, alveolar septa of the lung, and blood cells invading the liver parenchyma, whereas the pentagonal stars represent alveoli. The control group was given 200 μ L of distilled water by gavage, and the doses of F1, F2 and F3 administered were 10 mL/kg. Radar plots were generated via the bioinformatics platform (<http://www.bioinformatics.com.cn/>), and word cloud plots were generated via the flourish platform (<https://flourish.studio/examples/>)

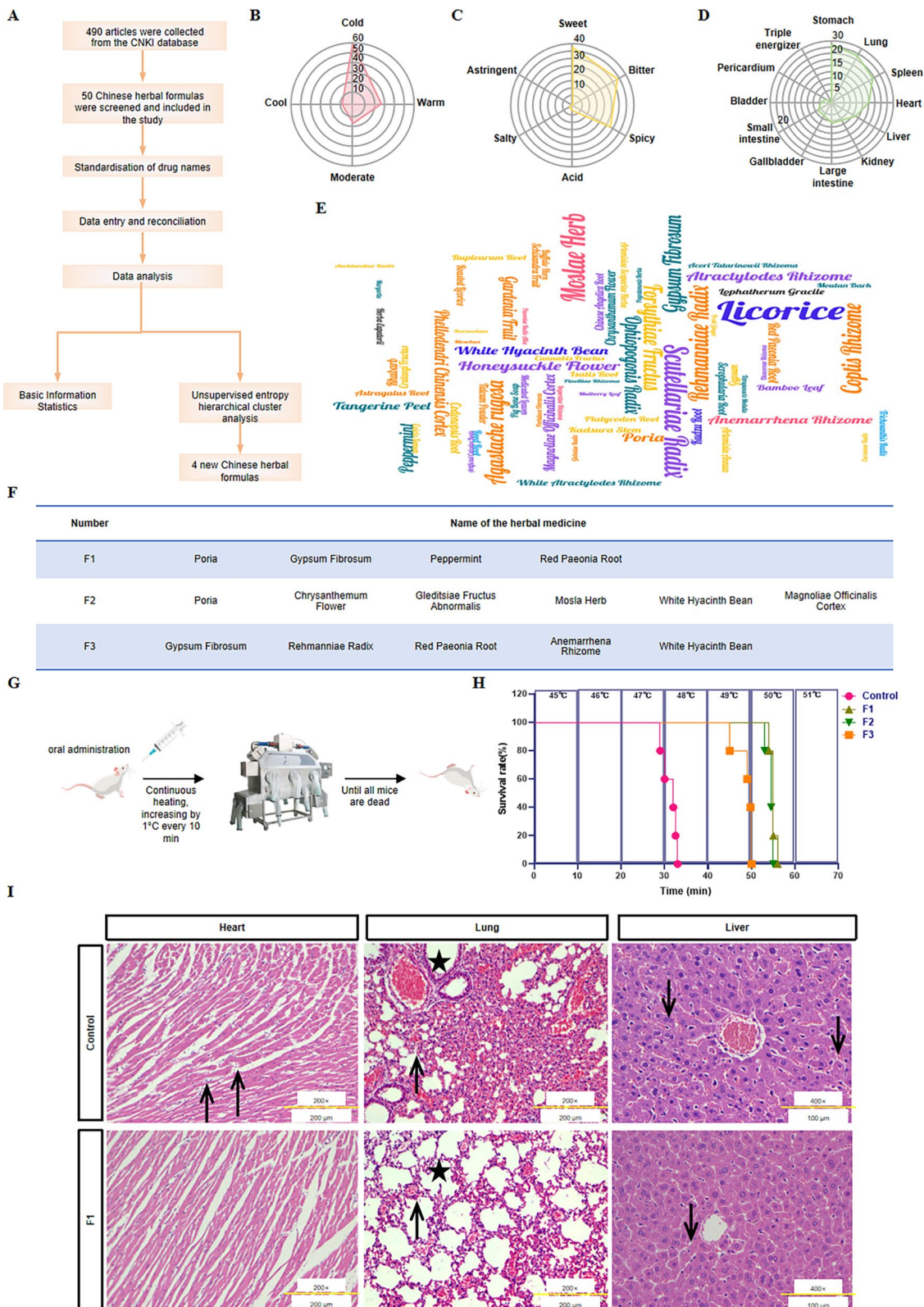


Fig. 1 (See legend on previous page.)

were weighed to exclude individual differences, and the results revealed that there was no significant difference between the weights of the broilers in each group (Fig. 2D). After the start of heat treatment, all broilers in the control group died at 60°C, whereas those in the SJD-L, SJD-M and SJD-H groups died completely at only 64, 65 and 66°C, respectively. These findings suggest that SJD has a good protective effect on broilers with acute heat stress in high-temperature and dry environments and that its anti-heat stress effect is concentration dependent, which implies that the higher the concentration of SJD signifies greater the anti-heat stress effect (Fig. 2F).

Induction of acute heat stress with high temperature and humidity to test the protective effect of SJD on Wenchang chickens

To simulate the summer high-temperature weather conditions in southern China, we referred to the weather changes in Wenchang (Hainan Province), a city in southern China, over the years. The extremely high temperature in Wenchang reached 34.2–38.7°C from April to September, and the humidity was approximately 84–87% (Fig. 2B). To expedite the test, we set the temperature at 45°C and maintained the humidity at 80–90%. After gavage administration of the drug, heat treatments were applied to the Wenchang chickens, and for this experiment, we maintained a constant temperature of 45°C and a fixed duration of 24 min to evaluate the anti-heat stress effect of the different treatments in terms of the survival rate of the chickens (Fig. 2C).

To determine the lowest effective dose of SJD, we administered 0.5%, 1% and 2% SJD stock solutions, referred to as SJD-L, SJD-M and SJD-H, respectively, and the administration of 0.025% vitamin C served as a positive control (Yin et al. 2020). The model and blank control groups were gavaged with equal volumes of distilled water, and finally, all broilers except those

in the blank control group were heat-treated. There was no significant difference in the pretreatment body weights of the broilers in each group (Fig. 2E). The survival rates of chickens in the model, positive control, and 0.5%, 1% and 2% SJD groups after heat treatment were 0%, 57.14%, 93.33%, 93.33% and 100%, respectively (Fig. 2G). Pathology revealed that chickens in the model group presented significant vacuolization and myocardial rupture of the heart; severe damage to the alveoli and significant hemorrhage in the liver and kidneys (indicated by arrows), whereas damage to the heart, lungs, liver, and kidneys was significantly alleviated in chickens in the positive control and SJD groups (Fig. 2H). The protective effect of SJD on organs was also significantly concentration dependent, with higher concentrations having greater effects on organ protection.

In conclusion, these results suggest that SJD has a better anti-heat stress effect even in high-temperature and humid environments, possibly because SJD may be able to protect the organs of chickens in these situations. In addition, the effective concentration of SJD should be greater than 2%, which can ensure a 100% survival rate of chickens under high-temperature shock.

Identification of the chemical constituents of SJD

After chromatographic separation and mass spectrometry data acquisition of the chemical constituents in SJD via UPLC–QTOF–MS, the data were processed on the basis of the theoretical mass spectrometry database of natural products in conjunction with the overall workflow of natural products in UniFi software, and the compositional information of SJD was obtained (Fig. 3A, B). The main active ingredients of SJD are muntjacoside E, timosaponin C, macrostemonoside H and mangiferin (Fig. 3C).

(See figure on next page.)

Fig. 2 Heat stress model of broilers to verify the anti-heat stress effect of SJD. Extreme high temperatures, extreme low temperatures and humidity in the (A) Turpan area and (B) Wenchang area in each month over the years. (C) Heat stress model of broilers with high-temperature, and dryness or humidity. (D) Body weights of broilers in each group before the experiment. (E) Body weights of the Wenchang chickens in each group before the experiment. (F) Survival rate of broilers under heat stress, $n = 10$. Control: control group, heat-treated and gavaged with distilled water. SJD-L: low-dose SJD group, heat-treated and gavaged with 1% SJD stock solution. SJD-M: medium-dose SJD group, heat-treated and gavaged with 10% SJD stock solution. SJD-H: high-dose SJD group, heat-treated and gavaged with 100% SJD stock solution. (G) Survival rate of Wenchang chickens under heat stress, $n = 10$. Blank: blank control group, no heat treatment, and gavage with distilled water. Model: Model group, heat treatment, and gavage with distilled water. Positive control: positive control group, heat treatment, and gavage with 0.025% vitamin C. SJD-L: low-dose SJD group, heat-treated, and gavage with 0.5% SJD. SJD-M: medium-dose SJD group, heat-treated, and gavaged with 1% SJD stock solution. SJD-H: high-dose SJD group, heat-treated, and gavaged with 2% SJD stock solution. SJD-H: high-dose SJD group, heat-treated, and gavaged with 2% SJD stock solution. (H) H&E staining of heart (200 \times , scale bar: 100 μ m), lung (200 \times , scale bar: 100 μ m), liver (100 \times , scale bar: 200 μ m) and kidney (200 \times , scale bar: 100 μ m) tissues from Wenchang chickens. Three chickens from each group were randomly selected for histological analysis, and six fields of view were randomly selected to capture images for each section. Representative data are shown. The downward arrows indicate sites of vacuolization and rupture in the heart muscle, and the upward arrows indicate sites of bleeding in the lungs, liver and kidneys

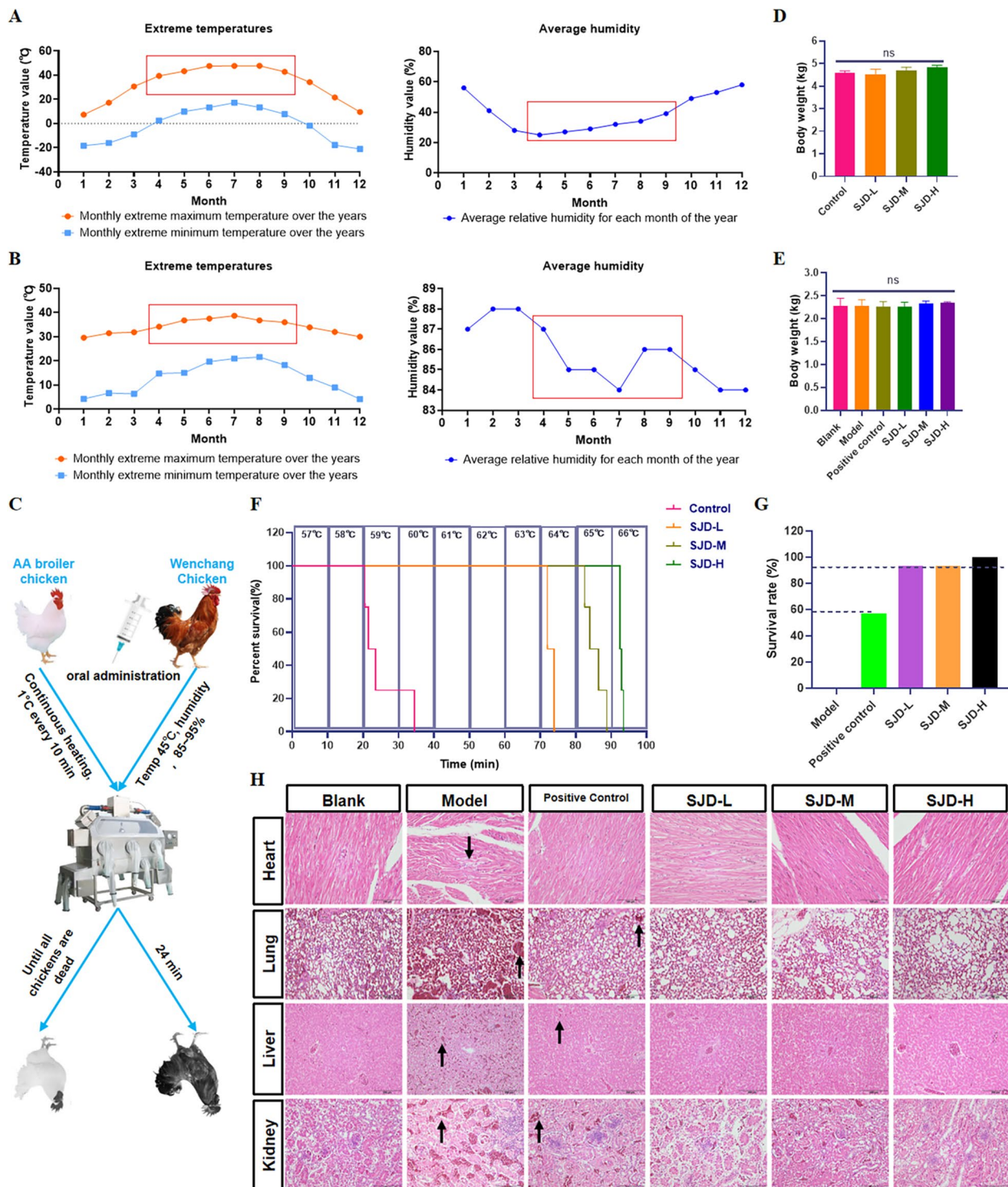


Fig. 2 (See legend on previous page.)

Analysis of the targets of SJD

In the theory of traditional Chinese medicine (TCM), heat stress is also known as ‘chi and yin deficiency’, which means a deficiency of ‘chi’ and ‘yin.’ Next, we explain the

main targets of SJD for the treatment of chi and yin deficiency with the help of TCM theory. Using the Swiss target prediction module of the Swiss ADME platform, we first predicted the top nine ingredients in SJD, with

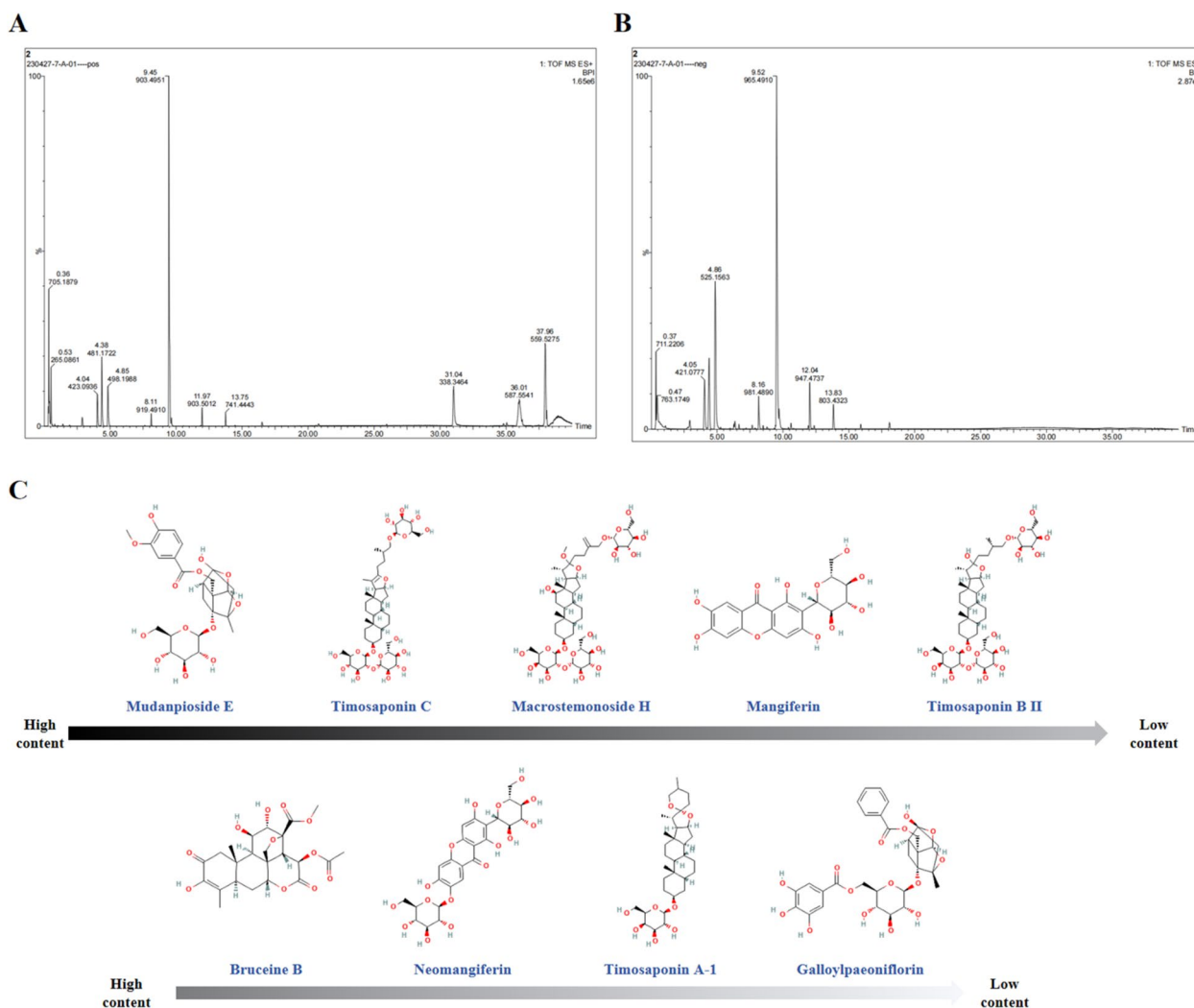


Fig. 3 Total ion current plot of SJD. **A** TIC diagram in positive ion mode. **B** TIC diagram in negative ion mode. **C** Top 9 ingredients in SJD

a total of 44 targets. We subsequently identified the targets related to ‘chi’ and ‘yin’ in the GeneCards and OMIM databases and identified the intersection of these three genes *via* a Venn diagram (Fig. 4A). The results revealed that 68 of the SJD therapeutic targets were related to chi and 66 were related to yin, resulting in a total of 50 targets common to all three. Therefore, we believe that these

50 targets are the most important targets for SJD treatment of chi and yin deficiency.

Protein-protein interactions were analyzed for these 50 targets *via* the STRING platform (Fig. 4B), and the protein-protein interaction (PPI) maps were redrawn *via* Cytoscape (V. 3.9.1) according to the level of the betweenness value. The circles of targets with higher

(See figure on next page.)

Fig. 4 Network pharmacology analysis. **A** Venn diagram of the top nine ingredient targets in SJD with chi- and yin-related targets. **B** Protein-protein interaction diagrams for 50 targets. **C** PPI diagram after sorting by betweenness. The inner circle indicates the most central target, and the larger and redder circles in the diagram represent greater betweenness values. **D** GO analysis. The 50 core targets were uploaded to the DAVID database for GO analysis. MF, molecular function; BP, biological process; CC, cell component. The top 10 results in terms of the number of enriched genes are shown. **E** KEGG analysis. The 50 core targets were uploaded to the DAVID database for pathway analysis, and the figure shows the top 30 pathways in terms of the number of enriched genes. The bubble plots shown were all generated *via* bioinformatics, with larger circles representing more enriched genes and redder colors representing lower *p* values

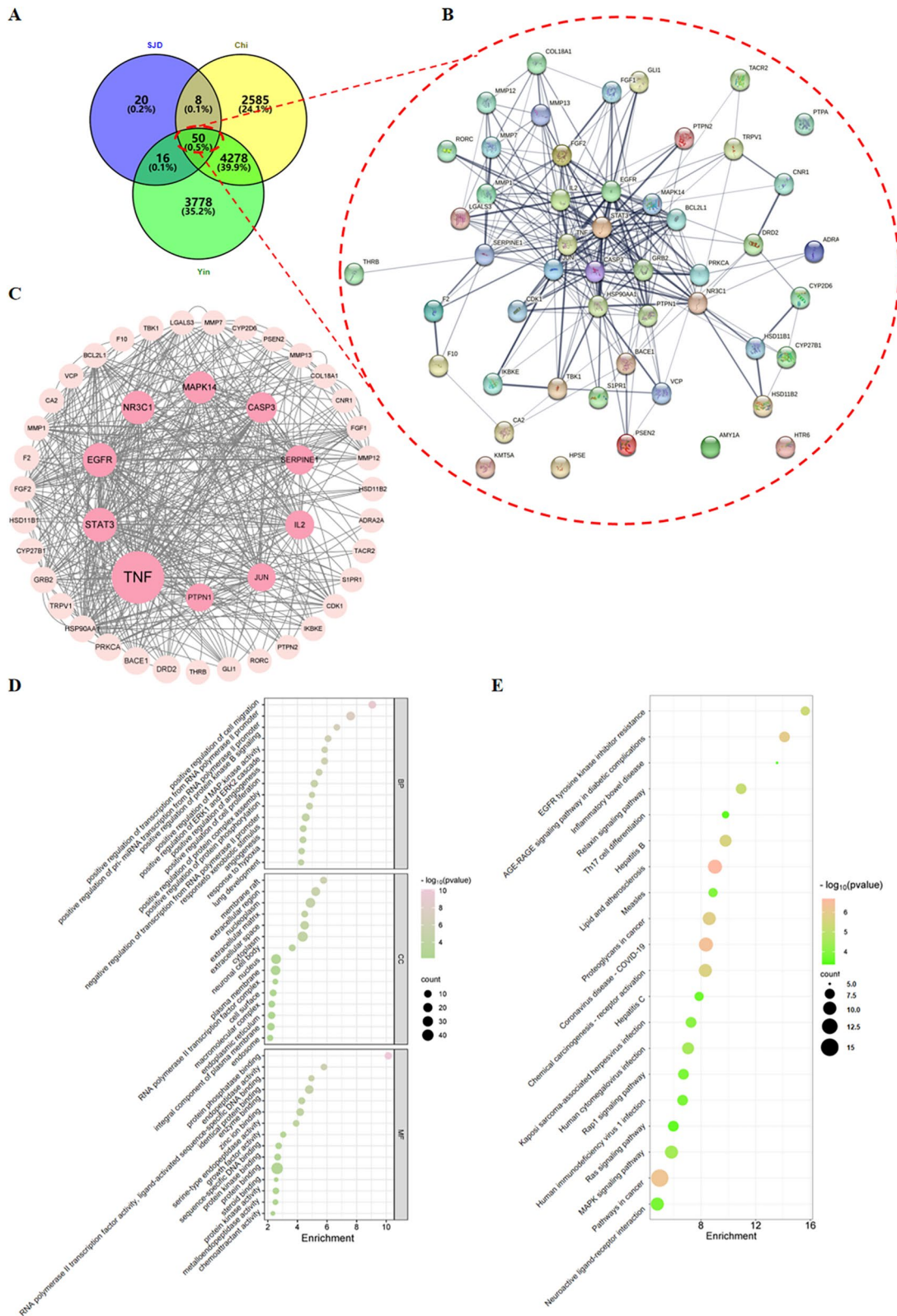


Fig. 4 (See legend on previous page.)

betweenness values were larger, indicating that the target occupied a more central position. The results revealed that the most central targets of SJD for the treatment of chi and yin deficiency were TNF, STAT3, EGFR and NR3C1, etc. (Fig. 4C).

GO and KEGG analysis

The genes corresponding to the above 50 targets were uploaded to the DAVID database for GO analysis. The results of the BP, CC and MF analyses were exported, and the first 15 results for each were generated. A bubble diagram of the GO enrichment results was generated via bioinformatics. The results revealed that these 50 genes were associated with biological processes such as positive regulation of cell migration, positive regulation of transcription from the RNA polymerase II promoter, and positive regulation of pri-miRNA transcription from the RNA polymerase II promoter (Fig. 4D). The main active ingredients of SJD may act on membrane rafts, extracellular regions, the nucleoplasm of the cell and other locations. The targets of SJD may be protein phosphatase binding, endopeptidase activity, RNA polymerase II transcription factor activity, and ligand-activated sequence-specific DNA binding.

KEGG pathway analysis was performed on the above 50 targets. The results revealed that the 50 overlapping target proteins were enriched in 80 pathways ($p < 0.05$), and the top 30 pathways were identified (Fig. 4E). The results revealed that the main active ingredient targets of SJD were closely related to resistance to EGFR tyrosine

kinase inhibitors and the AGE-RAGE signaling pathway in diabetic complications and inflammatory bowel disease.

Molecular docking

To evaluate the binding of the main active ingredients of SJD to target proteins, we selected the ingredients of SJD that can target TNF- α , STAT3, EGFR and nuclear receptor subfamily 3 group C member 1 (NR3C1) and performed molecular docking using SYBYL software (Table 1). A higher absolute value of the docking score indicates a higher probability that the ingredients bind to the target protein. The results revealed that the docking score of mudanpioside E with TNF- α was -7.1288. We used benpyrine and TNF-alpha-IN-2 (Ruan et al. 2021), two specific inhibitors of TNF- α , as controls, and the results revealed that the ability of mudanpioside E to specifically bind to TNF- α was greater than that of TNF-alpha-IN-2 but weaker than that of benpyrine. Mudanpioside E was able to form a hydrogen bond between Asn30 and Ala35 of the A chain of TNF- α (Fig. 5A).

The docking scores of timosaponin C, timosaponin B II and macrostemonoside H with STAT3 ranged from -8.2569 to -8.7870, whereas the docking scores of STAT3 with the two specific inhibitors static and cryptotanshinone were -5.8227 and -6.7568, respectively. These findings indicate that timosaponin C, timosaponin B II and macrostemonoside H specifically bind to STAT3 significantly better than the two specific inhibitors of STAT3, static and cryptotanshinone (Hou et al. 2023; Li et al. 2023c).

Table 1 Docking scores between the main active ingredients and key targets in SJD

PDB ID	Target	Expression location in cells	Ingredients	Docking score
1A8M	TNF- α	Cell membrane/Extracellular	Mudanpioside E	-7.1288
			^a Benpyrine	-8.2680
			^a TNF-alpha-IN-2	-2.9090
5AX3	STAT3	Cytoplasm/Nucleus	Timosaponin C	-8.2569
			Timosaponin B II	-8.3269
			Macrostemonoside H	-8.7870
			^b Static	-5.8227
			^b Cryptotanshinone	-6.7568
1IVO	EGFR	Cell membrane/Nucleus/Endoplasmic reticulum/Golgi apparatus membrane/Nuclear membrane	Timosaponin A I	-8.5874
			^c Tyrphostin B42	-6.77882
			^c Gefitinib	-7.9708
1M2Z	NR3C1	Cell nucleus/Cytoplasm/Mitochondria/Spindle/Centrosome/Cytoskeleton/Microstructural center	Chikusetsusaponin IVa	-8.2556
1A9U	MAPK14	Cytoplasm/Nucleus	Timosaponin A I	-7.4516
1CP3	CASP3	Cytoplasm	Chikusetsusaponin IVa	-7.3161

^a Specific inhibitor of TNF- α

^b Specific inhibitor of STAT3

^c Specific inhibitor of EGFR

Timosaponin A was able to form hydrogen bonds with amino acid residues such as Lys4, Leu225, Cys227 and Arg231 on the A chain of the EGFR protein (Fig. 5A). The docking scores were also significantly better than those of tyrphostin B42 and gefitinib, which are specific inhibitors of EGFR (Li et al. 2023a; Li et al. 2023b). These findings suggest that there may be greater binding potential between timosaponin A I and EGFR.

In conclusion, the above results suggest that several main active ingredients in SJD may have a strong binding capacity with targets such as TNF- α , STAT3 and EGFR.

Immunohistochemical analysis

Previously, we found that several main active ingredients of SJD specifically bind to the target proteins TNF- α , EGFR and STAT3 *via* molecular docking, but it is not clear whether they are agonists or inhibitors of TNF- α , EGFR and STAT3. Many previous studies have focused on damage to the heart during heat stress, with less attention given to the lungs. Therefore, we wanted to investigate the effects of SJD on the protein expression of TNF- α , p-EGFR and p-STAT3 in the lung tissue of Hainan Wenchang chickens *via* immunohistochemistry.

TNF- α is expressed mainly in the cell membrane and extracellular space. Immunohistochemistry revealed that in the lungs of control chickens, TNF- α was expressed only in small amounts near the microvessels (Fig. 5B), and in the model group, TNF- α was expressed in large amounts in the interstitial space of the lung tissues (indicated by the upward arrows). In the lung tissues of chickens gavaged before the high dose of SJD, the expression of TNF- α in the lung tissues was significantly lower than that in the model group.

Phosphorylated STAT3 (p-STAT3) is expressed in the cytoplasm, nucleus and lung tissues of Hainan Wenchang chickens and transmits extracellular signals to the nucleus through phosphorylation and dephosphorylation. Immunohistochemical results revealed that in the lungs of control chickens, p-STAT3 was expressed only in the cytoplasm of a small number of cells (Fig. 5B), whereas in the model group, p-STAT3 was expressed in large amounts in the cytoplasm and nucleus of the lung

tissue cells (indicated by the downward arrows), whereas the expression of p-STAT3 in the lung tissues was significantly lower than that in the model group after high-dose SJD gavage.

Phosphorylated EGFR (p-EGFR) is expressed on the cell membrane and transmits extracellular signals to the nucleus through phosphorylation and dephosphorylation. The immunohistochemistry results revealed that in the lungs of the control chickens, p-EGFR was expressed at low levels on the cell membranes (Fig. 5B), whereas in the model group, p-EGFR was abundantly expressed on the cell membranes of the lung tissues (indicated by the arrow to the left), whereas the expression of p-EGFR in the lung tissues was significantly lower than that in the high-dose pregavage group of SJD.

These results suggest that high-temperature treatment leads to a significant increase in the protein expression levels of TNF- α , p-EGFR and p-STAT3 in lung tissue, whereas SJD pregavage followed by heat treatment leads to a relative decrease in the protein expression levels of TNF- α , p-EGFR and p-STAT3. These findings suggest that SJD may inhibit the protein expression of TNF- α , p-EGFR and p-STAT3.

Oral acute toxicity assay

To assess the safety of wider oral administration of SJD, we conducted an acute oral toxicity study in rats in the present study. The rats were observed for 14 d following the oral administration of 30 g/kg over a 24 h period. The results revealed that both female and male rats survived with no abnormal symptoms, such as weight loss, unformed stools or abnormal behavior. Histological analysis revealed no significant lesions in the heart, liver, spleen, lung or kidney tissues of female or male rats (Fig. 5C), suggesting that SJD is not orally toxic.

Discussion

In the 21st century, heat stress caused by the intensification of extremely high-temperature climates around the globe not only posed a serious threat to human health but also aggravated animal husbandry. This study provides a systematic research model for the development and

(See figure on next page.)

Fig. 5 Molecular docking and immunohistochemistry results. **A** Three-dimensional binding of small molecules to target proteins and two-dimensional interactions are shown in the figure, and hydrogen bonding between small molecules and target proteins is shown in cyan. **B** Immunohistochemistry of Wenchang chicken lung tissue. The nuclei are shown in blue, and the brown areas indicate positive protein expression. The arrows indicate representative positive areas. The darker the brown color is, the higher the protein expression in that region. $n=6$. Three pathological sections were prepared for each chicken, and six fields of view were randomly selected from each section to capture images. 200 \times scale bar: 50 μ m, one-way ANOVA, ****: $p < 0.0001$; **: $p < 0.01$. **C** Results of H&E staining of heart, liver, spleen, lung and kidney tissues from female and male rats, $n=10$. Three pathological sections were prepared for each rat, and six fields of view were randomly selected to capture images for each section. Scale bars are 200 μ m. Heart, liver, lung and kidney tissues were imaged at 200 \times magnification, and spleen tissues were imaged at 100 \times magnification

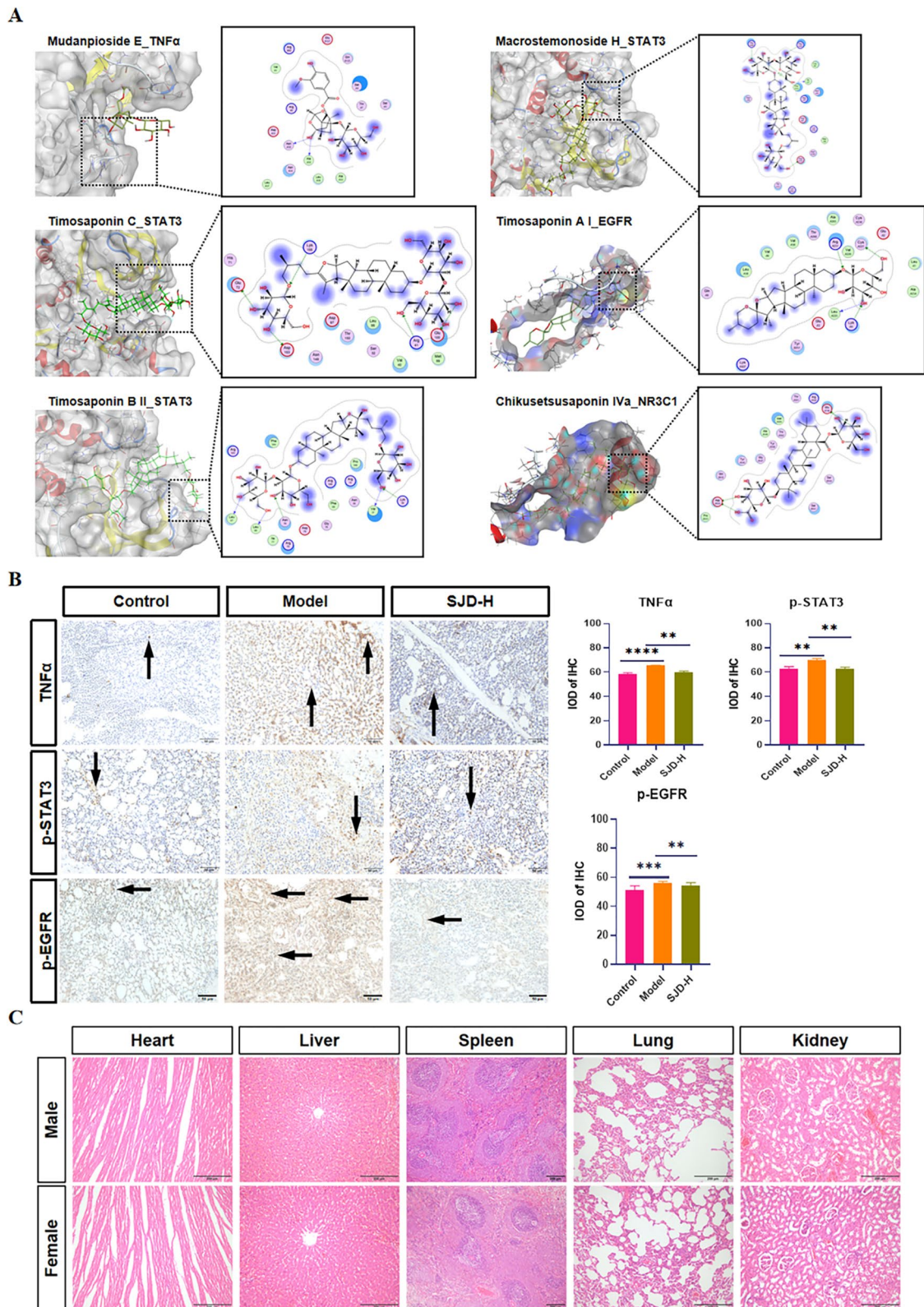


Fig. 5 (See legend on previous page.)

application of traditional Chinese medicine via big data analysis and network pharmacology (Fig. 6). To the best of our knowledge, the anti-heat stress CHF developed in this study has unprecedented anti-heat stress effects, significantly and quickly increasing the tolerance temperature by 2°C and 6°C in mice and chickens, respectively. Within 1 h of ingestion, the survival rate of chickens under acute heat stress can be increased to 100%.

This study suggests that SJD has promising application potential. Recent studies have shown that natural plant products, such as salidroside (extracted from *Rhodiola*), myricetin (a natural flavonoid from bayberry) and quercetin, which have protective effects against acute heat stress-induced myocardial damage, are effective against heat stress (Chen et al. 2019; Lin et al. 2017; Lin et al. 2018). However, these methods are still far from practical application. On the one hand, these natural products need to be taken at least 1 week in advance to be effective; on the other hand, these studies used conservative heat stress models, such as heating for 1 h a day for 7 d or continuous heating for 70 min, which are far from real environmental temperature changes. During the actual breeding process, summer heat waves often occur suddenly, far exceeding the temperature tolerance of the animals and resulting in sudden mortality. Therefore, the "gold standard" for evaluating the quality of acute heat stress medications is to determine whether they have an effect on mortality. Compared

with the reported medicine, SJD significantly and rapidly improves the temperature tolerance of the animals, with 100% survival rate of chickens under acute heat stress, making it more suitable for preventing acute heat stress at extremely high temperatures in summer. Furthermore, SJD has broader applicability because it can significantly improve the survival rate of broilers in high-temperature and high-humidity environments, which are more lethal to animals with no available and effective drugs (Asseng et al. 2021). When simulating the application of SJD, we considered the situation in which the humidity in summer is very different among different areas, such as Turpan and Wenchang. The results of this study show that SJD is resistant to acute heat stress in both dry and high-temperature environments and in humid and high-temperature environments, suggesting that SJD has wide potential for application.

The lungs and heart are likely the most important target organs for treating heat stress. Previous studies have shown that heat stress is a systemic response of organisms to a thermal environment that can cause damage to organs such as the heart, lungs, liver and kidneys (Chen et al. 2019). However, as shown in our previous studies of acute heat stress in chickens, we found that the lungs and heart undergo more dramatic and complex changes during acute heat stress (Nan et al. 2023). These findings suggest that the lungs and heart play a more important role in heat stress. In this study, we obtained new evidence

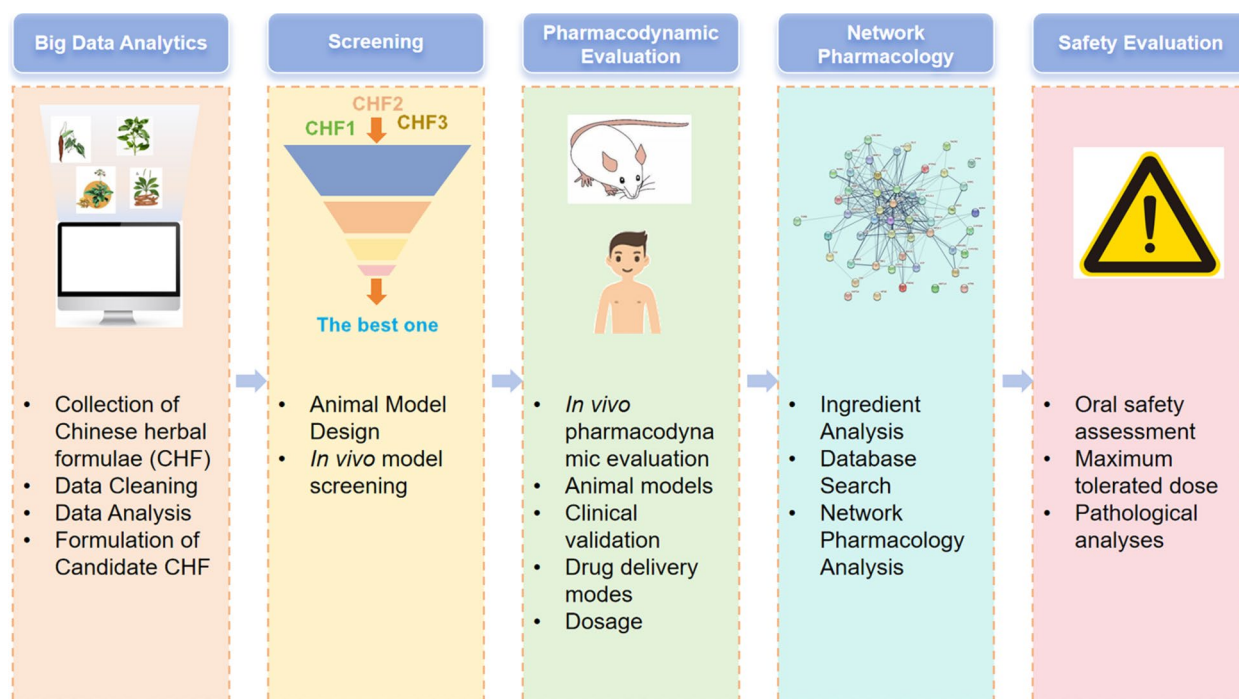


Fig. 6 A model for systematically developing new Chinese medicine formulations

when we analyzed the collected CHF and found that they tended to act on the organs of the lung, spleen and heart, suggesting that an anti-heat stress effect could be achieved by intervening in the lungs and heart. In heat stress models in mice and chickens, the lungs and heart are the most damaged organs under heat stress, with obvious structural damage, whereas the liver and kidney are infiltrated with only hemorrhagic and inflammatory cells. Similarly, SJD effectively protected the lungs and heart, reduced the damage caused by heat stress in both mice and chickens, and greatly improved the survival rate of both mice and chickens under heat stress. These results provide new insights for future research into heat stress. However, more research is needed to understand how the high-temperature environment damages the lungs and heart.

This study also provides a theoretical basis for the modern interpretation of the theory of 'chi and yin deficiency'. In the process of analyzing disease targets, we did not find heat stress-related targets directly but 'chi' and 'yin' related targets were found. On the one hand, pharmacological mechanism of SJD, a CHF, can be explained via TCM theory. On the other hand, we also hope to provide some new understanding of the modernization of traditional Chinese medicine theory in the process of studying SJD. In the theory of TCM, heat stress is also known as 'chi and yin deficiency'. In SJD, through big data analysis, *Gypsum fibrosum*, red Paeonia root, *Rehmanniae radix*, and *Anemarrhena rhizome* are known medicines that can counteract yin deficiency, whereas white hyacinth bean is believed to replenish chi. By identifying the ingredients of SJD and analyzing network pharmacology, we found that 58 of the 94 ingredients in SJD act on chi and that 66 of them act on yin. The targets of these compounds are closely related to life-based activities and material transformation, which is consistent with the TCM theory that yin represents the process of converting energy into matter and that chi is the process of exchange between yin and yang (Wang et al. 2020). In addition, through pathology analyses of the damage caused by heat stress or network pharmacology analyses of the targets of SJD, we have shown that inflammation results in traces, so the role of inflammation in 'chi' and 'yin' needs further research.

In addition to inflammatory factors (such as TNF α), we found for the first time that STAT3 and EGFR may play key roles in anti-heat stress. Signal transducer and activator of transcription (STAT) factors are involved in many processes, including early development, cell proliferation, survival and differentiation, and the response to inflammatory factors (Katturajan et al. 2022; Wei et al. 2023). The activation of EGFR stimulates a variety

of downstream pathways, including the Ras/MAPK, PI3K/AKT and JNK/STAT pathways, which regulate cell migration, proliferation and survival (Halder et al. 2023; Sadler et al. 2023; Sundqvist et al. 2020; Yang et al. 2019). In the present study, we first demonstrated via molecular docking that the active ingredients of SJD, timosaponin C, timosaponin B II and macrostemonoside H, can target STAT3 and that timosaponin A can target EGFR. We further demonstrated via immunohistochemistry that SJD exerts anti-thermal effects during heat stress by inhibiting EGFR and STAT3 phosphorylation. Considering that our validation of the binding of ingredients to targets is not yet sufficient, we compared the potential of ingredients of SJD with that of star inhibitors (such as tyrpstin B42, gefitinib, static and cryptotanshinone) in molecular docking to bind to these targets, providing a basis for the study of these targets and compounds. Nevertheless, the results of molecular docking are limited, and we are yet to ascertain the extent to which these compounds and target proteins bind in actual conditions, as well as their efficacy when acting independently. In the future, we will continue to investigate the effects of these ingredients and the role of these targets in heat stress.

Conclusion

The present study demonstrated the efficacy of SJD in preventing heat stress in poultry. The temperature tolerance of broilers increased by 6°C in both dry and humid high-temperature environments, and the survival rate of broilers at high temperatures was reported to be 100%. SJD is safe, nontoxic and can also be used to prevent heat stress. This study also provides new insights into the mechanisms of heat stress, revealing TNF- α , STAT3 and EGFR as potential targets for pharmacological intervention against heat stress. In conclusion, the present study not only developed a Chinese herbal formula, SJD, for the treatment of heat stress but also provided a theoretical basis for the development of anti-heat stress-targeted drugs in the future.

Methods

Reagents

Peppermint, Chrysanthemum flower, red paeonia root and other traditional Chinese medicine plants were purchased from Hubei Zhihetang Pharmacy Co. Ltd. (Wuhan, China); paraformaldehyde, n-butanol, anhydrous ethanol, xylene, hydrochloric acid, ammonia, xylene, and hydrogen peroxide were purchased from Sinopharm Chemical Reagent Co. Ltd. (Wuhan, China); methanol and formic acid were purchased from Thermo Fisher (Massachusetts, USA); deionized

water, prepared from Milli-Q Advantage A10 ultrapure water machine; HE staining solution, neutral dendrimer, citrate antigen repair solution and PBS buffer were purchased from Wuhan Bolf Biotechnology Co. Ltd. (Wuhan, China); DAB color development kits (K3468) were purchased from DAKO (Copenhagen, Denmark); HRP-conjugated secondary antibody (anti-rabbit, ab205718) and HRP-conjugated secondary antibody (anti-mouse, ab205719) were purchased from Abcam (Cambridge, UK); vitamin C (A8100), BSA (A8010), and rabbit serum (SL034) were purchased from Beijing Solarbio Technology Co. Ltd. (Beijing, China); rabbit anti-TNF- α antibody (bs-10802R), rabbit anti-STAT3 antibody (bs-1141R) and rabbit anti-EGFR antibody (bs-1644R) were purchased from Beijing Bioss Biotechnology Co. Ltd (Beijing, China).

Experimental animals

All animal experiments in this study were reviewed by the Scientific Ethics Committee of Huazhong Agricultural University (HZAU). Four- to five-week-old male KM mice (SPF grade), weighing 20 to 22 g, were purchased from the Animal Experimentation Centre of Huazhong Agricultural University with the ethics number HZAUMO-2022-0098; 6- to 8-week-old female and male SD rats (SPF grade), weighing 180 to 220 g, were purchased from Hunan SJA Laboratory Animal Co. Ltd. (Changsha City, Hunan Province), with the ethics number HZAURA-2023-0021; 15 to 18-day-old AA broiler chickens were purchased from Ezhou Lianghuchun Agricultural and Animal Husbandry Co. Ltd. (Ezhou City, Hubei Province); and 1-day-old Wenchang chickens (a breed of chicken in Wenchang, Hainan Province) were purchased from Hainan Taniu Wenchang Chicken Co. Ltd. (Haikou City, Hainan Province) and kept at the experimental chicken farm of Huazhong Agricultural University until 3 months after the start of the experiment. The ethical approval number of the chickens used in the experiments was HZAUCH-2022-0017.

Collection and analysis of traditional Chinese medicine prescriptions

The CHF patients included in this study were obtained from the China National Knowledge Infrastructure (CNKI) database via the searching of terms 'heat stress' and 'Chinese herbal formulas'. The search period was from 1 January 2001 to 1 October 2023 for literature on the treatment of heat stress in CHF patients. Articles related to the treatment of heat stress in CHF patients were reviewed, including articles containing expert experience and academic thinking on the treatment of heat stress in CHF patients,

as well as articles containing specific prescriptions for the treatment of heat stress or heat stroke. Articles that were not included in this study were theoretical discussions of Chinese medicine, review articles, self-reported empirical formulas with only the name, no specific drug composition or only a few Chinese herbs in the formula or no drug dosage and incomplete composition of formulas, dietary therapy articles, duplicate published articles (only one article was included), articles on the use of CHF in combination with other medicines, surgery, physiotherapy, topical medicines or acupuncture for the treatment of heat stress, articles on the efficacy of using Chinese medicine granules and ultramicro tablets instead of decocted Chinese medicine, articles on the efficacy of nonoral medicines (including acupuncture, external cleansing, postpressing and acupuncture injections), articles on the efficacy of ethnic minority medicines and articles on the addition of ethnic minority medicines to the main formulas and combinations of prescriptions.

The names of the CHF patients in the above articles have been standardized with reference to the Pharmacopoeia of the People's Republic of China (2020 Edition) (ChP), in which the same Chinese medicine with different parts of the body and different methods of preparation are considered one medicine if they have the same effect. According to the above criteria, the 'formulary management' module in the 'platform management system' of the Chinese Medicine Inheritance Auxiliary Platform (V2.5) (CMIAP) is selected, and the prescriptions are entered one by one. The input process adopts the way that two people input together to ensure the accuracy of the data, and after the prescription input is completed, the input data are checked again. After the prescriptions are entered, the 'Prescription Statistics' module of the CMIAP is entered, 'Basic Information Statistics' is selected, and the four natures, five flavors and meridian tropisms of the entered prescriptions are analyzed one by one. We select 'frequency statistics' and 'formulation law' in 'new formula analysis' to analyze the frequency of medicines, formulation laws and new formulas, respectively (Fig. 1A). Specifically, in this study, the number of support levels for the 'formulation law' was set to 10 (the number of support levels refers to the frequency of drug combinations that appear in all formulas). The support value of this parameter is 20% of the total number of formulas, i.e., support = 20%, number of supports = number of prescriptions multiply support), and the confidence level is set to 0.6. In the 'New Formulas Analysis', 'correlation' and 'penalty' were set to 7 and 3, respectively (the results of the system test showed that, in this study, 'correlation' and 'penalty' were set to 7 and 3, respectively, which are more desirable, and the results obtained are more satisfactory). For new prescriptions resulting from

the analysis, we will use our expertise to further evaluate the efficacy and safety of the prescriptions before conducting experimental screening.

Preparation of the herbal compound oral solution

The CHF_s were accurately weighed via an analytical balance, and each CHF was soaked in six times the volume of water ($v/m = 1:6$) for 20 min before extraction. Next, the herbs were continuously heated in a digital closed furnace (Changsha Mingjie Instrument Co., Ltd.) at 420°C until the water boiled, heated to 300°C for 35 min, and then filtered through eight layers of sterile gauze to obtain the first decoction. Next, six volumes of water were added to the dregs, which were boiled at 420°C, heated at 300°C for 25 min, and filtered through eight layers of sterile gauze to obtain the second decoction. The liquids obtained from the two decoctions were combined and concentrated at 350°C to a concentration of 1 g/mL.

Acute heat stress model in mice

Forty male KM mice were randomly divided into four groups of ten animals each after 7 d of adaptive feeding: the control, F1, F2 and F3 groups. The doses of CHF F1, F2 and F3 were calculated according to the formulas for converting the human dose to the mouse dose in the 'Techniques for the Study of Traditional Chinese Medicines':

$$\text{Dosage administered to mice (mg/kg)} \times 3 = \text{Dosage administered to humans (mg/kg)} \times 37$$

The mice were fasted for 12 h before heat treatment, and normal water intake was maintained. The control group was given 200 μ L of distilled water by gavage, the doses of F1, F2 and F3 were 10 mL/kg, and heat treatment was performed 1 h after the administration of F1, F2 and F3. Specifically, the mice were placed in an isolator and heated from 45°C to observe whether they died; if they did not die, the temperature was continuously increased, and the temperature was maintained at the same level for 10 min for each 1°C increase. Finally, the survival rate of the mice in each group was calculated until all the mice had died. Heart, lung and liver tissues from the mice in the longest survival group and the control group were collected and fixed in 4% paraformaldehyde.

Dry heat stress model of dry heat in broilers

Forty broilers were randomly divided into control, high-dose, medium-dose and low-dose groups, for a total of four groups with ten birds in each group. There was no significant difference in the average body weight of the broilers in each group. The broilers in each group were fasted for 12 h before heat treatment, and the drug was administered by gavage in a volume of 1 mL of distilled

water in the control group, 1 mL of the original SJD solution in the high-dose (SJD-H) group, 10% of the SJD solution in the medium-dose (SJD-M) group and 1% of the SJD solution in the low-dose (SJD-L) group. Heat treatment was performed 1 h after drug administration. Heating was performed in an isolation chamber, starting at 57°C (referring to the pretest results), and the humidity was maintained at 25–35%, with temperature increasing 1°C every 10 min until all the birds died. The survival rates at different time intervals were calculated.

Damp heat stress model of Wenchang chickens

Ninety Wenchang chicken birds were divided into six groups of fifteen birds in each group. After 7 d of acclimatization, heat treatment was started. One day before the treatment, the chickens were fasted for 12 h. Then, 1 h before the start of heat treatment, the chickens in the other groups, except those in the blank control group and the model group, were given the corresponding concentrations of vitamin C and SJD by gavage. In the blank control and model groups, chickens were gavaged with 10 mL of distilled water; in the positive control group, chickens were gavaged with 10 mL of 0.025% vitamin C; and in the experimental group, chickens were gavaged with 10 mL of 0.5%, 1% and 2% SJD (1 g/mL). The blank control group did not undergo heat treatment, and the other groups were heat-treated. The temperature of

the isolation chamber was adjusted to 45°C, the humidity was adjusted to 80–90%, and heat treatment was carried out for 24 min, during which the conditions of the chickens were closely monitored (referring to the pretest results). At the end of the experiment, five live chickens were randomly selected from each group to be slaughtered, and the liver, kidney, lung, and heart tissues were collected and fixed with 4% paraformaldehyde.

UPLC-QTOF-MS analysis

After the SJD oral mixture was freeze-dried into solid particles, 5 g of SJD was added, 10 mL of 50% methanol aqueous mixture (v/v , methanol:water = 1:1) was added for dissolution, the mixture was ultrasonicated for 30 min, 1 mL of the supernatant was added to a centrifuge tube, the mixture was centrifuged at 14,000 rpm for 5 min, the supernatant was filtered through a 0.22 μ m micropore filter membrane, and the mixture was then injected into the vials for UPLC-QTOF-MS analysis.

UPLC-MS/MS analysis was performed on a Waters UPLC (I-Class)-MS (XEVO-G2QTOF) liquid mass spectrometry system using a Waters ACQUITY UPLC BEH-C18 column (1.8 μ m \times 2.1 mm \times 100 mm). The column

temperature was set at 40°C, and the sample injection volume was set at 5 µL. The flow rate was set to 0.3 mL/min. The mobile phase consisted of 0.1% formic acid aqueous solution (A) and 0.1% formic acid acetonitrile solution, and a multistep linear gradient elution procedure was used. During each acquisition cycle, the mass acquisition range was 50–1,500 Da, the spray voltage was 3.0 kV (positive) or -2.7 kV (negative), the capillary temperature was 400°C, the sheath gas flow rate was 800 L/h, and the auxiliary gas flow rate was 50 L/h. UNIFI database software was used to match the methods (Table 2).

Network pharmacological analysis

On the basis of the compositional assay results above, the top 9 active ingredients in SJD were screened out, and they were searched in the PubChem database (<https://pubchem.ncbi.nlm.nih.gov/>) to download the 2D model and canonical SMILES of each compound (Kim et al. 2019). Using the Swiss target prediction module of the Swiss ADME platform (<http://www.swisstargetprediction.ch/>), the canonical SMILES of each compound was imported to obtain the predicted target and common name of each compound (Daina et al. 2019).

The potential targets related to ‘chi’ (or ‘qi’) and ‘yin’ were collected from the GeneCards database (<https://www.genecards.org/>) and the OMIM database (<https://www.omim.org/>). Venn diagrams were used to intersect the targets of SJD action with those related to ‘chi’ and ‘yin’ diseases to obtain the intersecting targets of SJD and chi and yin. The targets were uploaded to the String platform (<https://cn.string-db.org/>) for visual mapping to obtain protein-protein interaction (PPI) information (Crosara et al. 2018). With Cytoscape (V. 3.9.1) software, the overlapping targets and predicted related targets were queried via the CytoNCA plug-in to obtain the betweenness value, which was used as a reference for further screening and mapping of the core targets. The overlapping genes were imported into the DAVID database (<https://david.ncifcrf.gov/>). The algorithm selected was ‘Official-Gene-Symbol’, and the associated data from the biological process (BP), cell component (CC), molecular function (MF) and Kyoto Encyclopedia of Genes and Genomes (KEGG) categories were exported (Kanehisa

et al. 2019; Shen et al. 2021). The results of the BP, CC and ME categories of the top 15 terms in the Gene Ontology (GO) analysis were visualized in a horizontal bar graph with a color gradient in bioinformatics (<http://www.bioinformatics.com.cn/>), and all pathways in the KEGG pathway analysis were visualized in a bubble diagram.

Molecular docking validation

The 3D structures of the proteins were obtained from the Protein Data Bank (PDB) database (<https://www1.rcsb.org/>), the 3D structures of the compounds were obtained from the PubChem database, and molecular docking was performed via SYBYL (Trepco Corporation, USA). After the protein docking environment was prepared, docking pockets were discovered via the Site Finder mode, compounds were imported into SYBYL, induced fit was selected, and the number of docking attempts was set to 60 to display only the highest-scoring results.

Histological analysis

The preparation of tissue sections consisted of gradient dehydration of paraformaldehyde-fixed tissues, followed by paraffin embedding and sectioning with a microtome. For H&E staining, the sections were first immersed in xylene twice for 20 min each, then in anhydrous ethanol and 75% ethanol for 5 min each, and finally washed with distilled water. The sections were then stained with hematoxylin for 5 min and washed with distilled water. This was immediately followed by treatment with 1% hydrochloric acid in water for 3 s and then washing with distilled water. The tissue was immersed in 0.7% ammonia for 3 s, washed with distilled water, dehydrated in a gradient of 85% ethanol and 95% ethanol, and finally stained with eosin for 5 min. The excess stain was washed off with distilled water, and the tissue was immersed in anhydrous ethanol three times for 5 min each, followed by n-butanol for 5 min and xylene for 5 min in that order. The sections were air-dried and then blocked in neutral resin.

For the IHC-stained sections, the procedure for dewaxing was the same as that described above, and the sections were washed with distilled water and then placed in a repair cassette filled with citrate antigen repair buffer (pH 6.0) for antigen repair in a microwave oven for 8 min while the medium was heated until boiling. Then, the mixture was allowed to warm for 8 min and switched to medium-low heat for 7 min to prevent excessive buffer evaporation. After natural cooling, the slides were washed in phosphate buffer solution (PBS, pH 7.4) on a decolorization shaker three times for 5 min each. Then, the sections were incubated in 3% hydrogen peroxide solution for 25 min at room temperature, protected from light, and then washed in PBS (pH 7.4)

Table 2 Gradient elution conditions

Time	FlowRate (mL/min)	%A	%B
0	0.3	98	2
9	0.3	0	100
12	0.3	0	100
13	0.3	98	2
15	0.3	98	2

on a decolorization shaker three times for 5 min each to block endogenous peroxidase activity. The sections were shaken dry, coverslipped evenly with 3% bovine serum albumin (BSA) and sealed for 30 min at room temperature. The sealing solution was gently shaken, the primary antibody diluted in PBS was added to the sections, and the sections were incubated flat in a wet box at 4°C overnight. The next day, the sections were placed on a destaining shaker in PBS (pH 7.4) three times for 5 min each to block endogenous peroxidase. On the following day, the sections were washed three times in PBS (pH 7.4) on a decolorizing shaker for 5 min each time, dried, covered with a secondary antibody (HRP-conjugated) of the same genus as the primary antibody and incubated for 50 min at room temperature. The color development time was monitored under a microscope, and development was stopped by rinsing the sections with tap water when the positive color was brownish-yellow. The sections were incubated with hematoxylin for approximately 3 min, rinsed with tap water, differentiated with hematoxylin differentiation solution for a few seconds, rinsed with tap water, returned to blue with hematoxylin blue return solution and rinsed with running water. The sections were sequentially placed in 75% alcohol and 85% alcohol for 5 min each, and then the process was repeated in anhydrous ethanol and xylene twice for 5 min each. The sections were then removed from the xylene to dry slightly and were sealed with neutral gum. The prepared sections were analyzed under a microscope (BX53, Olympus Corporation, Japan).

Acute oral toxicity test

The experiment started after 7 days of acclimatization. Ten female and ten male rats were used in the experiment. The rats were fasted for more than 16 h before dosing, and the total dose was 30.0 g/kg. Three doses were administered at intervals of 1 h. The rats were observed once before dosing, closely observed for 3 h after dosing, and then further observed for 14 days. The mortality rates of the rats and the conditions of the skin, fur, eyes, mucous membranes, secretions, and excretions, as well as changes in respiration, circulation, and the autonomic and central nervous systems, were recorded. Presence symptoms such as tremors, convulsions, salivation, diarrhea, lethargy and coma were observed. At the end of the test, necropsies were performed on all surviving animals and those that were found dead during the test. During necropsy, the body surfaces of the animals were visually inspected for abnormalities in all body orifices, head, chest, abdomen, pelvis, etc., and their contents were recorded. Vital organs such as the heart, liver, spleen and lungs were examined for lesions, and tissue sections were prepared for further examination.

Data analysis

All the data in this study were analyzed with GraphPad Prism (8.0.2) via one-way ANOVA. The values are expressed as the means \pm standard errors. Image visualization was performed through platforms such as bioinformatics, Flourish and Venny 2.1.

Abbreviations

BP	Biological process
BSA	Bovine serum albumin
CC	Cell component
ChP	Pharmacopoeia of the People's Republic of China
CMIAP	Chinese Medicine Inheritance Auxiliary Platform
CHF	Chinese herbal formula
CNKI	China National Knowledge Infrastructure
EGFR	Epidermal growth factor receptor
GO	Gene ontology
HZDP	Huoxiang Zhengqi Dropping Pills
KEGG	Kyoto Encyclopedia of Genes and Genomes
LC-ADCP	Lead center for annual-to-decadal climate prediction
MF	Molecular function
ROS	Reactive oxygen species
PBS	Phosphate buffer solution
PDB	Protein data bank
PPI	Protein-protein interaction
SJD	Shidi Jieshu Decoction
STAT3	Signal transducer and activator of transcription 3
TCM	Traditional Chinese medicine
TNF- α	Tumor necrosis factor α
UPLC/MS	Ultra-performance liquid chromatography/mass spectrometry
WMO	World Meteorological Organization

Acknowledgments

We would like to thank Proof Reading Service.com Ltd. for providing proof-reading services (PRS) for this article.

Authors' contributions

HF: Conceptualization, data curation, formal analysis, investigation, methodology, software, visualization, writing – original draft; SY: Investigation, methodology, validation; HY and BY: Investigation, validation; YP and AI: Resources, writing – review & editing; SJ and XW: Funding acquisition, project administration, resources, supervision, writing – review & editing.

Funding

This work was supported by the Major Special Science and Technology Plan (202302AA310020), the National Natural Science Foundation of China (NSFC) (32072925, 32473087) and the National Student Innovation and Entrepreneurship Training Program of Huazhong Agricultural University (202310504018).

Data availability

The relevant data and material in this article are available and can be requested from the corresponding authors.

Declarations

Ethics approval and consent to participate

All animal experiments in this study were authorized by the Animal Experimentation Centre of Huazhong Agricultural University, and the ethical numbers of the different animal experiments can be found in the Materials and Methods section.

Competing interests

The authors declare that they have no competing interests.

Author details

¹National Reference Laboratory of Veterinary Drug Residues (HZAU) and MAO Key Laboratory for the Detection of Veterinary Drug Residues, Huazhong Agricultural University, Wuhan 430070, Hubei, China. ²Key Laboratory

of Agricultural Animal Genetics, Breeding and Reproduction, Ministry of Education, Huazhong Agricultural University, Wuhan 430070, Hubei Province, China. ³Department of Biosciences, COMSATS University Islamabad, Sahiwal Campus, Islamabad 45550, Pakistan. ⁴Key Laboratory of Smart Farming for Agricultural Animals, Ministry of Education, Huazhong Agricultural University, Wuhan 430070, Hubei Province, China. ⁵Hubei Hongshan Laboratory, Wuhan 430070, Hubei Province, China.

Received: 4 September 2024 Accepted: 10 October 2024

Published online: 08 November 2024

References

- Asseng, S., P. Martre, A. Maiorano, R.P. Rotter, G.J. O'Leary, G.J. Fitzgerald, C. Girousse, R. Motzo, F. Giunta, M.A. Babar, et al. 2019. Climate change impact and adaptation for wheat protein. *Glob. Change Biol.* 25 (1): 155–173. <https://doi.org/10.1111/gcb.14481>.
- Asseng, S., D. Spankuch, I.M. Hernandez-Ochoa, and J. Laporta. 2021. The upper temperature thresholds of life. *Lancet Planet. Health* 5 (6): e378–e385. [https://doi.org/10.1016/S2542-5196\(21\)00079-6](https://doi.org/10.1016/S2542-5196(21)00079-6).
- Chen, G., H. Fan, and J. Zhu. 2019. Salidroside pretreatment protects against myocardial injury induced by heat stroke in mice. *J. Int. Med. Res.* 47 (10): 5229–5238. <https://doi.org/10.1177/0300060519868645>.
- Crosara, K., E.B. Moffa, Y. Xiao, and W.L. Siqueira. 2018. Merging in-silico and in vitro salivary protein complex partners using the string database: a tutorial. *J. Proteomics* 171 (16): 87–94. <https://doi.org/10.1016/j.jprot.2017.08.002>.
- Dadgar, S., E. Greene, A. Dhamad, B. Mallmann, S. Dridi, and N. Rajaram. 2021. Diffuse reflectance spectroscopy reveals heat stress-induced changes in hemoglobin concentration in chicken breast. *Sci. Rep.* 11 (1): 3649. <https://doi.org/10.1038/s41598-021-83293-y>.
- Daina, A., O. Michielin, and V. Zoete. 2019. Swisstargetprediction: updated data and new features for efficient prediction of protein targets of small molecules. *Nucleic. Acids. Res.* 47 (W1): W357–W364. <https://doi.org/10.1093/nar/gkz382>.
- Desta, T.T. 2021. The genetic basis and robustness of naked neck mutation in chicken. *Trop. Anim. Health Prod.* 53 (1): 95. <https://doi.org/10.1007/s11250-020-02505-1>.
- Fathi, M.M., A. Galal, L.M. Radwan, O.K. Abou-Emera, and I.H. Al-Homidan. 2022. Using major genes to mitigate the deleterious effects of heat stress in poultry: an updated review. *Poult. Sci.* 101 (11): 102157. <https://doi.org/10.1016/j.psj.2022.102157>.
- Godde, C.M., D. Mason-D'Croz, D.E. Mayberry, P.K. Thornton, and M. Herrero. 2021. Impacts of climate change on the livestock food supply chain; A review of the evidence. *Glob Food Secur Agric Policy* 28: 100488. <https://doi.org/10.1016/j.jgs.2020.100488>.
- Gomez-Pastor, R., E.T. Burchfiel, and D.J. Thiele. 2018. Regulation of heat shock transcription factors and their roles in physiology and disease. *Nature Reviews. Molecular Cell Biology* 19 (1): 4–19. <https://doi.org/10.1038/nrm.2017.73>.
- Gonzalez-Rivas, P.A., S.S. Chauhan, M. Ha, N. Fegan, F.R. Dunshea, and R.D. Warner. 2020. Effects of heat stress on animal physiology, metabolism, and meat quality: a review. *Meat Sci.* 162: 108025. <https://doi.org/10.1016/j.meatsci.2019.108025>.
- Halder, S., S. Basu, S.P. Lall, A.K. Ganti, S.K. Batra, and P. Seshacharyulu. 2023. Targeting the EGFR signaling pathway in cancer therapy: what's new in 2023? *Expert Opin. Ther. Targets* 27 (4–5): 305–324. <https://doi.org/10.1080/14728222.2023.2218613>.
- Hamilton, T., A. Siqueira, L.S. de Castro, C.M. Mendes, J.C. Delgado, P.M. de Assis, L.P. Mesquita, P.C. Maiorka, M. Nichi, M.D. Goissis, J.A. Visintin, and M. Assumpcao. 2018. Effect of heat stress on sperm DNA: protamine assessment in ram spermatozoa and testicle. *Oxidative Med. Cell. Longev.* 2018 (25): 5413056. <https://doi.org/10.1155/2018/5413056>.
- Hou, X.X., Y.W. Li, J.L. Song, W. Zhang, R. Liu, H. Yuan, T.T. Feng, Z.Y. Jiang, W.T. Li, and C.L. Zhu. 2023. Cryptotanshinone induces apoptosis of activated hepatic stellate cells via modulating endoplasmic reticulum stress. *World J. Gastroenterol.* 29 (17): 2616–2627. <https://doi.org/10.3748/wjg.v29i17.2616>.
- Kanehisa, M., Y. Sato, M. Furumichi, K. Morishima, and M. Tanabe. 2019. New approach for understanding genome variations in KEGG. *Nucleic. Acids. Res.* 47 (D1): D590–D595. <https://doi.org/10.1093/nar/gky962>.
- Katturajan, R., S. Nithiyandam, M. Parthasarathy, A.V. Gopalakrishnan, E. Sathiyamoorthi, J. Lee, T. Ramesh, M. Iyer, S.E. Prince, and R. Ganesan. 2022. Immunomodulatory role of thioredoxin interacting protein in cancer's impediments: current understanding and therapeutic implications. *Vaccines* 10 (11): 1902. <https://doi.org/10.3390/vaccines10111902>.
- Kim, S., J. Chen, T. Cheng, A. Gindulyte, J. He, S. He, Q. Li, B.A. Shoemaker, P.A. Thiessen, B. Yu, L. Zaslavsky, J. Zhang, and E.E. Bolton. 2019. Pubchem 2019 update: improved access to chemical data. *Nucleic. Acids. Res.* 47 (D1): D1102–D1109. <https://doi.org/10.1093/nar/gky1033>.
- Li, Y., H. Tao, J. Hong, Y. Xiong, X. Pan, Y. Liu, X. Yang, and H. Zhang. 2022. The chinese herbal formula huoxiang zhengqi dropping pills prevents acute intestinal injury induced by heatstroke by increasing the expression of claudin-3 in rats. *Evid.-Based Complement Altern. Med.* 2022: 1–11. <https://doi.org/10.1155/2022/9230341>.
- Li, G., S. Liu, Y. Chen, J. Zhao, H. Xu, J. Weng, F. Yu, A. Xiong, A. Udduttula, D. Wang, P. Liu, Y. Chen, and H. Zeng. 2023a. An injectable liposome-anchored teriparatide incorporated gallic acid-grafted gelatin hydrogel for osteoarthritis treatment. *Nat. Commun.* 14 (1): 3159. <https://doi.org/10.1038/s41467-023-38597-0>.
- Li, J., X. Wu, X.B. Ji, C. He, S. Xu, and X. Xu. 2023b. Biphasic function of GSK3 β in gefitinib-resistant NSCLC with or without EGFR mutations. *Exp. Ther. Med.* 26 (4): 488. <https://doi.org/10.3892/etm.2023.12187>.
- Li, X., Y. Wang, Z. Zhai, Q. Mao, D. Chen, L. Xiao, S. Xu, Q. Wu, K. Chen, Q. Hou, Q. He, Y. Shen, M. Yang, Z. Peng, S. He, X. Zhou, H. Tan, S. Luo, C. Fang, G. Li, and T. Chen. 2023c. Predicting response to immunotherapy in gastric cancer via assessing perineural invasion-mediated inflammation in tumor microenvironment. *J. Exp. Clin. Cancer Res.* 42 (1): 206. <https://doi.org/10.1186/s13046-023-02730-0>.
- Lin, X., C. Lin, T. Zhao, D. Zuo, Z. Ye, L. Liu, and M. Lin. 2017. Quercetin protects against heat stroke-induced myocardial injury in male rats: antioxidative and antiinflammatory mechanisms. *Chem. Biol. Interact.* 265 (1): 47–54. <https://doi.org/10.1016/j.cbi.2017.01.006>.
- Lin, X., T. Zhao, C.H. Lin, D. Zuo, Z. Ye, S. Lin, S. Wen, L. Liu, M.T. Lin, C.P. Chang, and C.M. Chao. 2018. Melatonin provides protection against heat stroke-induced myocardial injury in male rats. *J. Pharm. Pharmacol.* 70 (6): 760–767. <https://doi.org/10.1111/jphp.12895>.
- Ma, B., L. Zhang, J. Li, T. Xing, Y. Jiang, and F. Gao. 2021. Heat stress alters muscle protein and amino acid metabolism and accelerates liver gluconeogenesis for energy supply in broilers. *Poult. Sci.* 100 (1): 215–223. <https://doi.org/10.1016/j.psj.2020.09.090>.
- Mora, C., C. Counsell, C.R. Bielecki, and L.V. Louis. 2017. Twenty-seven ways a heat wave can kill you: deadly heat in the era of climate change. *Circ Cardiovasc Qual Outcomes* 10 (11): e004233. <https://doi.org/10.1161/CIRCOUTCOMES.117.004233>.
- Mu, D., H. Li, D. Wang, X. Yang, and S. Wang. 2022. Analysis of environmental and social significant factors affecting the flow of maternal patients in jilin. *China. Front. Public Health* 10 (9): 780452. <https://doi.org/10.3389/fpubh.2022.780452>.
- Munguia, G.G., A.C. Brooks, S.A. Thomovsky, E.J. Thomovsky, A. Rincon, and P.A. Johnson. 2024. Emergency approach to acute seizures in dogs and cats. *Vet. Sci.* 11 (6): 277. <https://doi.org/10.3390/vetsci11060277>.
- Nan, J., H. Yang, L. Rong, Z. Jia, S. Yang, and S. Li. 2023. Transcriptome analysis of multiple tissues reveals the potential mechanism of death under acute heat stress in chicken. *Bmc Genomics* 24 (1): 459. <https://doi.org/10.1186/s12864-023-09564-2>.
- Nawab, A., F. Ibtisham, G. Li, B. Kieser, J. Wu, W. Liu, Y. Zhao, Y. Nawab, K. Li, M. Xiao, and L. An. 2018. Heat stress in poultry production: mitigation strategies to overcome the future challenges facing the global poultry industry. *J. Therm. Biol.* 78: 131–139. <https://doi.org/10.1016/j.jtherbio.2018.08.010>.
- Pernas, S., A. Fernandez-Novo, C. Barrajon-Masa, P. Mozas, N. Perez-Villalobos, B. Martin-Maldonado, A. Oliet, S. Astiz, and S.S. Perez-Garnelo. 2023. Bull semen obtained on beef farms by electroejaculation: sperm quality in the first two hours of storing with different extenders and holding temperatures. *Animals* 13 (9): 1561. <https://doi.org/10.3390/ani13091561>.

- Ruan, S., L. Zhai, S. Wu, C. Zhang, and Q. Guan. 2021. SCFAs promote intestinal double-negative T cells to regulate the inflammatory response mediated by NLRP3 inflammasome. *Aging (Albany Ny)* 13 (17): 21470–21482. <https://doi.org/10.18632/aging.203487>.
- Sadler, K.V., J. Bowes, C.F. Rowlands, C. Perez-Becerril, C.M. van der Meer, A.T. King, S.A. Rutherford, O.N. Pathmanaban, C. Hammerbeck-Ward, S. Lloyd, et al. 2023. Genome-wide association analysis identifies a susceptibility locus for sporadic vestibular schwannoma at 9p21. *Brain*. 146 (7): 2861–2868. <https://doi.org/10.1093/brain/awac478>.
- Saeed, M., G. Abbas, M. Alagawany, A.A. Kamboh, M.E. Abd El-Hack, A.F. Khafaga, and S. Chao. 2019. Heat stress management in poultry farms: a comprehensive overview. *J. Therm. Biol.* 84: 414–425. <https://doi.org/10.1016/j.jtherbio.2019.07.025>.
- Sedaghatmehr, M., V.P. Thirumalaikumar, I. Kamranfar, K. Schulz, B. Mueller-Roeber, A. Sampathkumar, and S. Balazadeh. 2021. Autophagy complements metalloprotease FtsH6 in degrading plastid heat shock protein HSP21 during heat stress recovery. *J. Exp. Bot.* 29: erab304. <https://doi.org/10.1093/jxb/erab304>.
- Sejian, V., R. Bhatta, J.B. Gaughan, F.R. Dunshea, and N. Lacetera. 2018. Review: adaptation of animals to heat stress. *Animal* 12 (s2): s431–s444. <https://doi.org/10.1017/S1751731118001945>.
- Shakeri, M., J.J. Cottrell, S. Wilkinson, H.H. Le, H. Suleria, R.D. Warner, and F.R. Dunshea. 2019. Growth performance and characterization of meat quality of broiler chickens supplemented with betaine and antioxidants under cyclic heat stress. *Antioxidants* 8 (9): 336. <https://doi.org/10.3390/antiox8090336>.
- Shen, X., H. Li, W. Zou, J. Wu, L. Wang, W. Wang, H. Chen, L. Zhou, Y. Hu, X. Qin, and J. Yang. 2021. Network pharmacology analysis of the therapeutic mechanisms underlying beimu-gualou formula activity against bronchiectasis with in silico molecular docking validation. *Evid-Based Complement Altern Med* 2021 (5): 1–17. <https://doi.org/10.1155/2021/3656272>.
- Sundqvist, A., E. Vasilaki, O. Voytyuk, Y. Bai, M. Morikawa, A. Moustakas, K. Miyazono, C.H. Heldin, D.P. Ten, and H. van Dam. 2020. TGF β and EGF signaling orchestrates the AP-1- and p63 transcriptional regulation of breast cancer invasiveness. *Oncogene* 39 (22): 4436–4449. <https://doi.org/10.1038/s41388-020-1299-z>.
- Surai, P.F., I.I. Kochish, V.I. Fisinin, and M.T. Kidd. 2019. Antioxidant defence systems and oxidative stress in poultry biology: an update. *Antioxidants* 8 (7): 235. <https://doi.org/10.3390/antiox8070235>.
- Umemura, Y., H. Ogura, H. Matsuura, T. Ebihara, K. Shimizu, and T. Shimazu. 2018. Bone marrow-derived mononuclear cell therapy can attenuate systemic inflammation in rat heatstroke. *Scandinavian Journal of Trauma, Resuscitation and Emergency Medicine* 26 (1): 97. <https://doi.org/10.1186/s13049-018-0566-2>.
- van Wettere, W., K.L. Kind, K.L. Gatford, A.M. Swinbourne, S.T. Leu, P.T. Hayman, J.M. Kelly, A.C. Weaver, D.O. Kleemann, and S.K. Walker. 2021. Review of the impact of heat stress on reproductive performance of sheep. *J. Anim. Sci. Biotechnol.* 12 (1): 26. <https://doi.org/10.1186/s40104-020-00537-z>.
- Vandana, G.D., V. Sejian, A.M. Lees, P. Pragna, M.V. Silpa, and S.K. Maloney. 2021. Heat stress and poultry production: impact and amelioration. *Int. J. Biometeorol.* 65 (2): 163–179. <https://doi.org/10.1007/s00484-020-02023-7>.
- Wang, C., X. Wang, T. Tao, D. Song, J. Wang, Y. Wang, X. Liu, and X. Wu. 2020. Traditional chinese medicines alleviated myocardial ischemia by regulating qi and promoting blood circulation. *J Tradit Chin Med.* 40 (6): 974–982. <https://doi.org/10.19852/j.cnki.jtcm.2020.06.009>.
- Wei, W., J. Wang, P. Huang, S. Gou, D. Yu, and L. Zong. 2023. Tumor necrosis factor-alpha induces proliferation and reduces apoptosis of colorectal cancer cells through STAT3 activation. *Immunogenetics* 75 (2): 161–169. <https://doi.org/10.1007/s00251-023-01302-y>.
- Wickramasuriya, S.S., E. Kim, H.M. Cho, T.K. Shin, B. Kim, M. Lee, S. Seo, J.M. Heo, and H. Choi. 2019. Differential effects of dietary methionine isomers on broilers challenged with acute heat stress. *J. Poultry Sci.* 56 (3): 195–203. <https://doi.org/10.2141/jpsa.0180072>.
- Yang, L., S. Lin, Y. Kang, Y. Xiang, L. Xu, J. Li, X. Dai, G. Liang, X. Huang, and C. Zhao. 2019. Rhein sensitizes human pancreatic cancer cells to egfr inhibitors by inhibiting STAT3 pathway. *J. Exp. Clin. Cancer Res.* 38 (1): 31. <https://doi.org/10.1186/s13046-018-1015-9>.
- Yin, B., L. Di, S. Tang, and E. Bao. 2020. Vitamin CNa enhances the antioxidant ability of chicken myocardium cells and induces heat shock proteins to relieve heat stress injury. *Res. Vet. Sci.* 133: 124–130. <https://doi.org/10.1016/j.rvsc.2020.09.008>.
- Zheng, Y., T. Xie, S. Li, W. Wang, Y. Wang, Z. Cao, and H. Yang. 2021. Effects of selenium as a dietary source on performance, inflammation, cell damage, and reproduction of livestock induced by heat stress: a review. *Front. Immunol.* 12 (18): 820853. <https://doi.org/10.3389/fimmu.2021.820853>.

Publisher's Note

Springer Nature remains neutral with regard to jurisdictional claims in published maps and institutional affiliations.